JTTEE5 17:136–143
DOI: 10.1007/s11666-007-9150-4
1059-9630/$19.00 © ASM International

Peer Reviewed

High-temperature Oxidation Behavior and Surface Roughness Evolution of VPS NiCrAlY Coating

D. Seo, K. Ogawa, T. Shoji, and S. Murata

(Submitted February 19, 2007; in revised form July 16, 2007)

In this work, as a background to the development of high temperature environmental protection coating technology, the structural transformation of vacuum-plasma sprayed NiCrAlY coating has been studied, including the oxidation behavior, elastic modulus, microhardness, and surface roughness. Coating was oxidized isothermally at a 1,273 K for different time periods up to 1,000 h in order to form the oxide scale layer. The results showed that the oxide scale and weight gain increased proportional to the exposure time. The surface roughness and hardness decreased after isothermal exposure, but they are not proportional to the exposure time. The oxide scale growth was concentrated in the valleys of the surface at the early 1 h exposure (decreasing surface roughness), whereas the oxide scales over a longer perspective (time period), grew on the convex surface (increasing surface roughness).

Keywords Degradation, Isothermal oxidation, NiCrAlY, VPS

1. Introduction

High temperature environmental protection coatings are designed from the understanding of oxidation and hot corrosion processes that have been developed over the last half century (Ref 1-5). The oxidation of metals depends on the rates at which anion or cation transport can occur through the crystal lattice or along grain boundaries in the oxide (Ref 6). Many attempts have been made to further improve scale adhesion, oxidation/corrosion resistance, and obtain strain-tolerant scales by modifying the MCrAlY alloy composition and spraying methods (Ref 7-10). Protective alumina scales are the basis for the oxidation resistance of many high temperature material systems including metallic overlay coatings, superalloys, and thermal barrier coating (TBC) systems. A thin, continuous scale of adherent, slow-growing Al_2O_3 provides an effective diffusion barrier that protects the underlying metal from deleterious oxidation (Ref 11). Residual stresses generated by a combination of scale-growth stresses and thermal-expansion mismatches with the metallic substrate often result in cracking, buckling, and spallation of these brittle oxide films, which accelerates the degradation of overlay coatings. Since many high-temperature metallic components (e.g., superalloy hardware in gas turbine engines) experience severe thermal cycles, it is important to understand the scale response to thermo-mechanical stresses in order to design alloys that form protective oxides with optimized spallation resistance. Stresses in thin oxide films are difficult to measure and the fracture behavior of alumina scales on overlays is not well understood (Ref 12), mainly due to variations in scale microstructures, flaws, and interfacial adhesion as a function of the substrate chemistry, mechanical properties, and surface condition. In addition, there has been relatively little detailed microstructural investigations of the evolution phenomenon of thermally grown oxide (TGO) accumulation on protective overlay coatings after isothermal oxidation (Ref 13-15), because spallation and sintering of the damaged scales often complicates or prevents such an analysis. An improved understanding of the microstructures, flaws, and fracture behavior of Al_2O_3 scales grown under isothermal conditions must be attained before a basis for the long-term structure-properties relationships of these protective oxide layers can be developed.

2. Experimental

The substrate material selected in this study was commercially available Inconel 718, which is widely used for gas turbine components, with a chemical composition of 19Cr-19Fe-5.1Nb-3Mo-0.9Ti-0.5Al-balance Ni (wt.%). The substrates were polished and grit-blasted with alumina powder (grit 60) before being vacuum plasma

D. Seo, K. Ogawa, and **T. Shoji**, Fracture & Reliability Research Institute, Tohoku University, Aoba 6-6-01, Aramaki, Aoba-ku, Sendai 980-8579, Japan; and **S. Murata**, Murata Boring Technology Research Co., Ltd., Kitamaruko 1-30-45, Suruga-ku, Shizuoka 421-0106, Japan. Contact e-mail: seodw@rift.mech.tohoku.ac.jp.

sprayed (VPS). Commercially available argon atomized NiCrAlY spraying powder (Praxair NI-343, USA), with a chemical composition of 67.1Ni-21.9Cr-10Al-0.9Y in wt.% was used in this study. The nominal particle size was −45/+10 μm (D_{50}: 18.5 μm), and the average thickness of the as-sprayed coating was 340 ± 11 μm. The VPS processes were carried out under the following conditions: preheating temperature 843 K during transferred arc treatment, voltage 56-57 V, current 580-590 A, spraying distance 310 mm, argon gas atmosphere 8 kPa. To characterize the oxidation behavior, static oxidation experiment was carried out in air under isothermal conditions at 1,273 K up to 1,000 h. Each exposure condition consisted of approximately 32 K/min heating rate in a kanthal muffle furnace, and approximately 3 K/min cool-down to ambient temperature. The aim of this oxidation procedure was to create accelerated conditions for testing. Weight change measurement was made at the end of each time interval with the help of an electronic balance (Sartorius LA120S, Germany) with a sensitivity of 0.1 mg. The substrate was removed by grinding with SiC abrasive paper to leave only the overlaid NiCrAlY coating. And then the detached freestanding coating was polished to the final 0.5 μm alumina finish before the weight gain measurements, to minimize the difference in the effective surface area between the each side of specimen. After thermal exposure, the oxidized samples were analyzed by the energy dispersive X-ray (EDX) analysis with scanning electron microscopy (SEM; Hitachi S-4700, Japan) for the element profile of surface area (150 × 100 μm). The samples were then cut and mounted for the cross-sectional analysis. The TGO and coating thickness were measured by taking a back-scattered electron image (BSEI) with the SEM, equipped with a Robinson back scattered detector (RBSD). More than 15 points were measured for each sample and the average value of the thickness was chosen. The microhardness (H) of coating including a substrate was measured by a computer-controlled measuring system using the load versus indentation depth method according to ISO 14577-1 (Fischerscope HM2000 XYp, Germany). A 500 mN load was provided to the needle for penetration and the indenter is a diamond Vickers pyramid with 136° plane angle. Taking into account the geometric relationship between the indentation depth and the shape of the indenter, this measurement produces the physically meaningful Martens hardness HM $= F/A$, where F is a test load and A is a surface area of penetration. The Vickers values (H_v) were converted from the corresponding indentation hardness according to ISO 14577-1. The elastic modulus (E) was also computed automatically from the recorded measurement plot, calculated on the basis of the slope of the tangent on the unloading curve with $F = F_{max}$. The mean H_v values were taken by measuring seven points on the splats approximately 100 μm depth from the coating surface, and the load resolution was ≤ 40 μN and the penetration depth resolution was ≤ 100 pm. The surface roughness of coatings was measured by the contactless measuring system (Mitaka NH-3T, Mitaka Kohki. Co., Japan). This system had the auto-focusing laser probe with the 3-dimensional resolution of 0.1 × 0.1 × 0.01 μm.

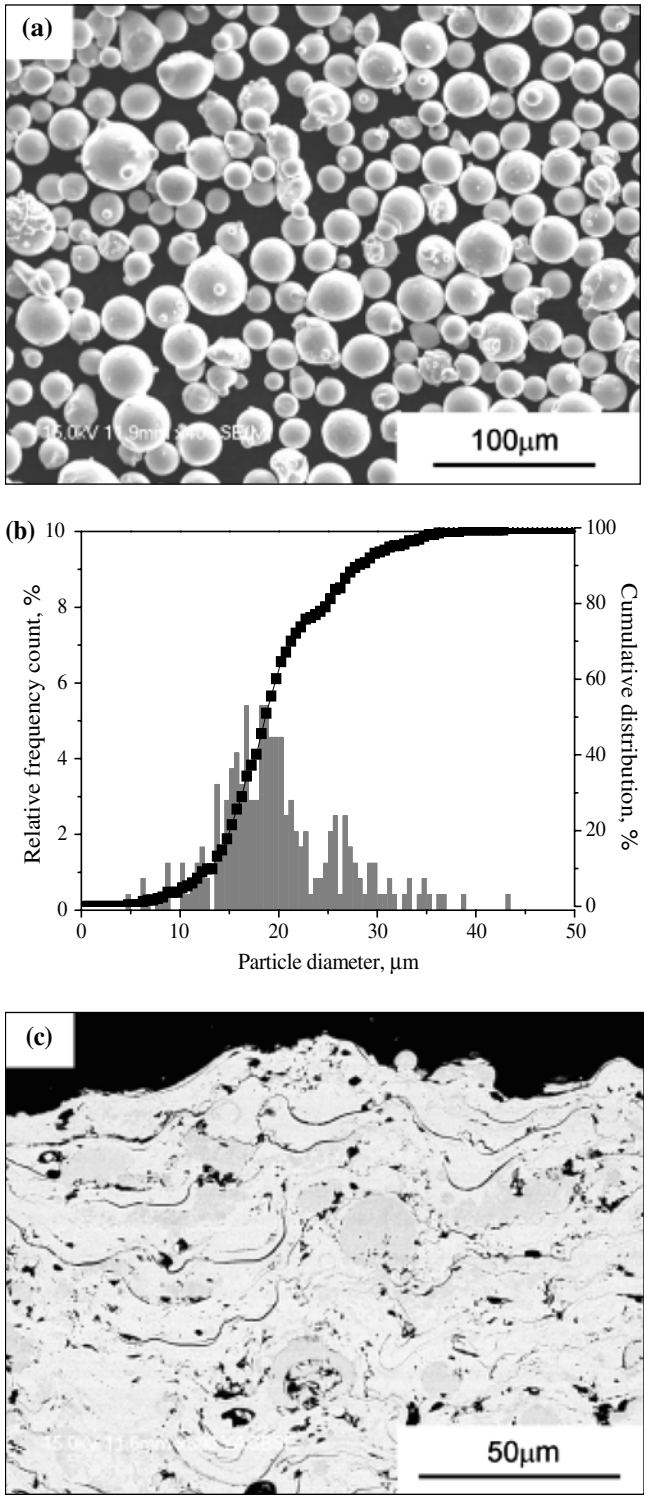

Fig. 1 Powder (a) morphology and (b) size distribution; and (c) microstructure of as-sprayed coating

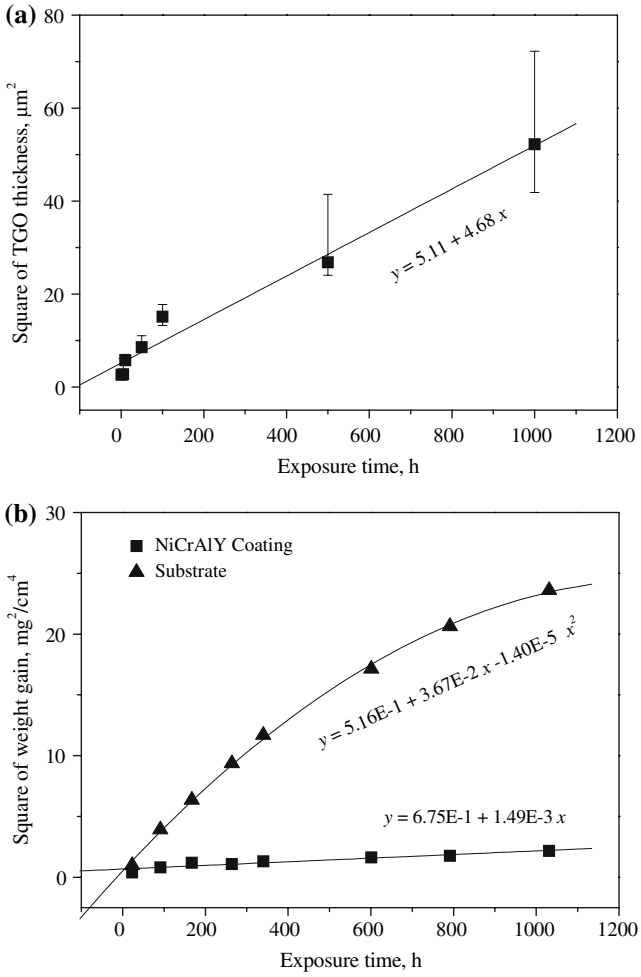

Fig. 2 Oxidation kinetics of VPS NiCrAlY coating; (a) TGO thickness growth of coating; (b) weight gain of coating and substrate

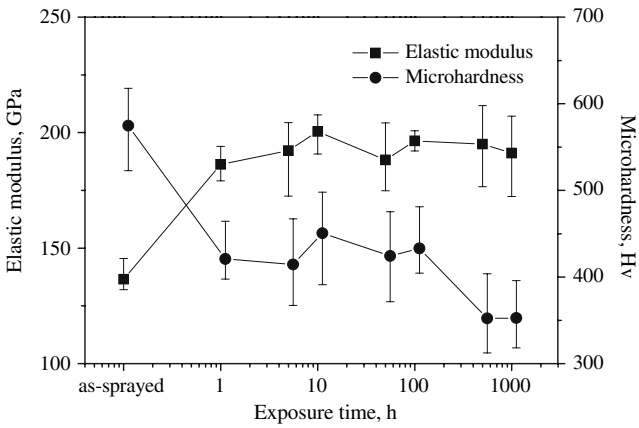

Fig. 3 Elastic modulus and microhardness profiles of VPS NiCrAlY coating

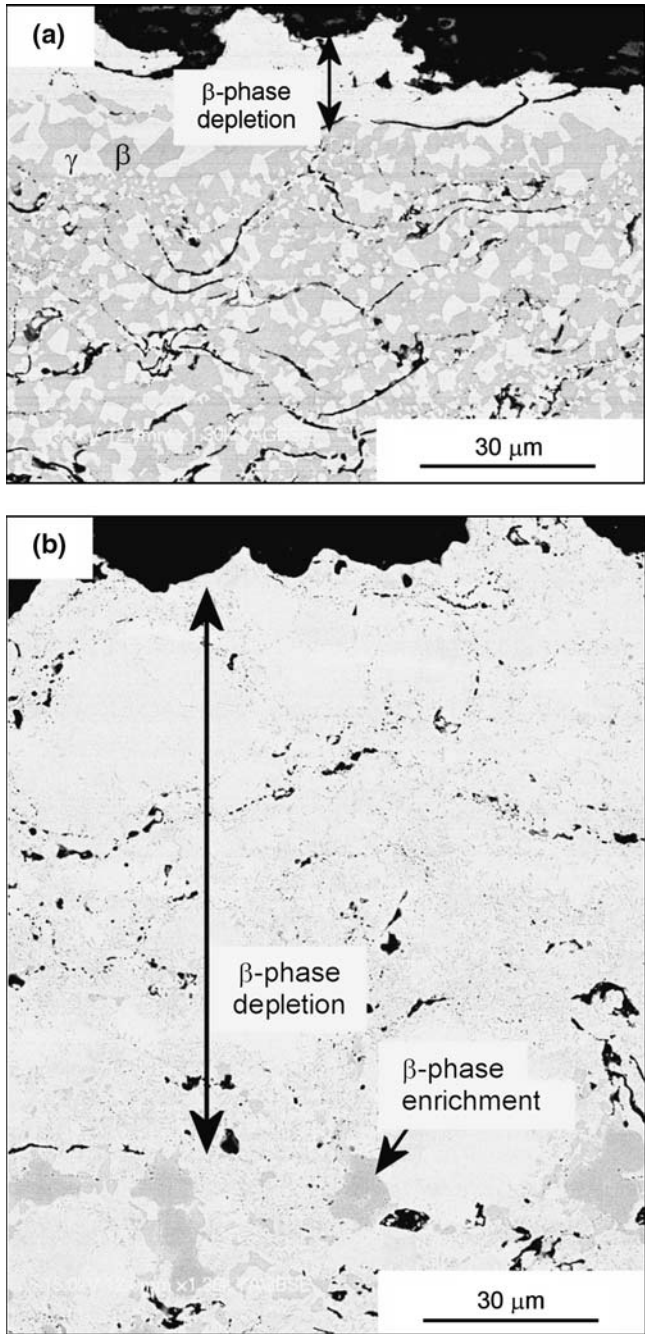

Fig. 4 BSE images of β-phase depletion after (a) 100 h and (b) 500 h thermal exposure

3. Results and Discussion

3.1 Morphology and TGO Growth

Figure 1(a) shows the typical morphology of spray powder used in this study. The powder has a spherical shape. The distribution of the particle size; measured using SEM images, is shown in Fig. 1(b). From the

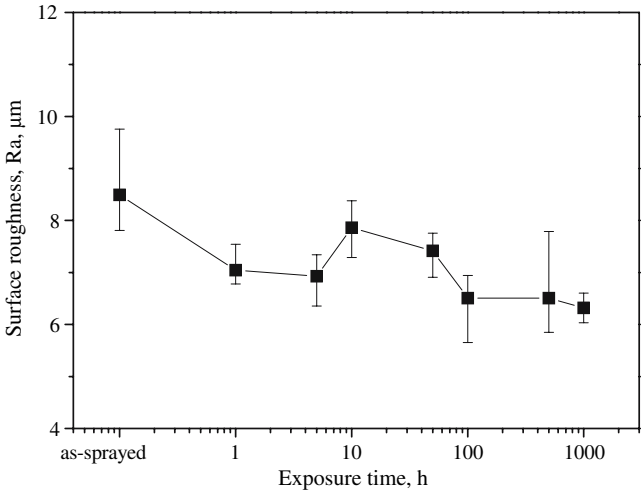

Fig. 5 Surface roughness of NiCrAlY coating with increased thermal exposure time

cross-sectional microstructures of the sprayed coating (on substrate) shown in Fig. 1(c), some voids and oxide inclusions can be seen inside coating. The microstructure also included some partially unmelted particles and showed a laminar structure with irregular shape.

The TGO thickness and weight gain plots of the NI-343 coating and the substrate without coating in static air at 1,273 K are shown in Fig. 2. Both plots of coatings exhibited a tendency to have the increasing TGO thickness growth and weight gain with increasing exposure time after an initially higher rate of oxidation, i.e., they followed the parabolic rate law of oxidation between TGO thickness (or weight gain) and exposure time. In case of the coating, the square value of TGO thickness is proportional to the exposure time; the square of the weight gain is also proportional to the exposure time. In this oxidation process, the parabolic rate constant can be derived for the units relating to measurement of the oxide thickness as the reaction parameter. There are several methods of following the reaction, depending on choice of reaction parameter, each of which produces its own particular parabolic rate constant, using Wagner's notation for the various parabolic rate constants (Ref 1). The parabolic oxidation rate constant is generally defined by the equation $(\Delta W/A)^2 = k''t$ where ΔW is the weight change at any time, A is the surface area, t is time, and k'' is the scaling constant using measurement of the mass increase of the specimen. In case of TGO thickness growth, the kinetics of the scale thickness growth can be represented by the modified equation $x^2 = 2k't$ where x is the scale thickness, t is time, and k' is the scaling constant using measurement of scale thickness. The parabolic rate constant k' is 2.34×10^{-2} μm^2 h^{-1} ($R = 2.91$E−18), and the constant k'' is 1.49×10^{-3} mg^2 cm^{-4} h^{-1} ($R = 1.94$E−4) for NI-343 coating, respectively. But the Inconel 718 substrate does not follow an exact parabolic rate law, this is due to the rapid scale growth in the transient oxidation stage (below 340 h) (Ref 1).

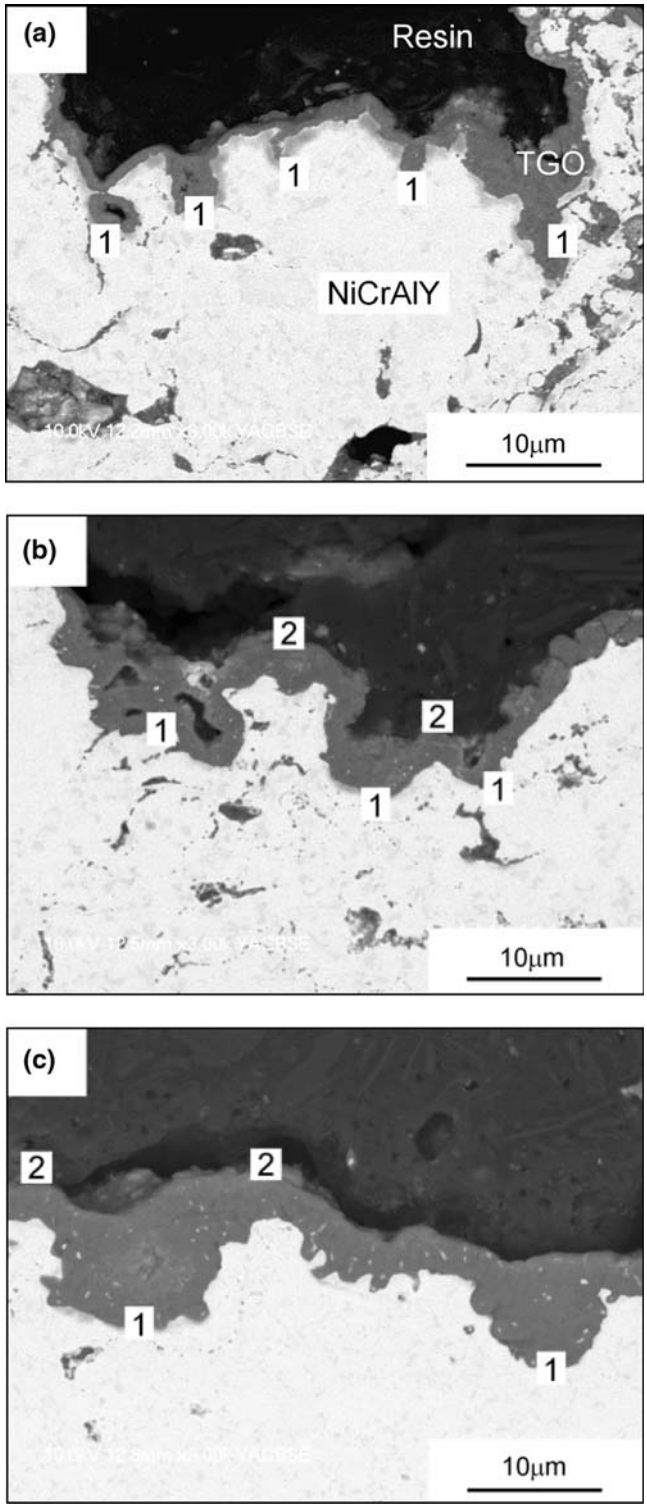

Fig. 6 Evolution of surface roughness after thermal exposure for (a) 1 h, (b) 10 h and (c) 100 h: TGO scales are filled into the concave surfaces (point 1) at first step, and then grow on the convex surfaces (point 2)

The microhardness was gradually decreased according to increase of exposure time as shown in Fig. 3. This may be due to the microstructural and phase transformation of

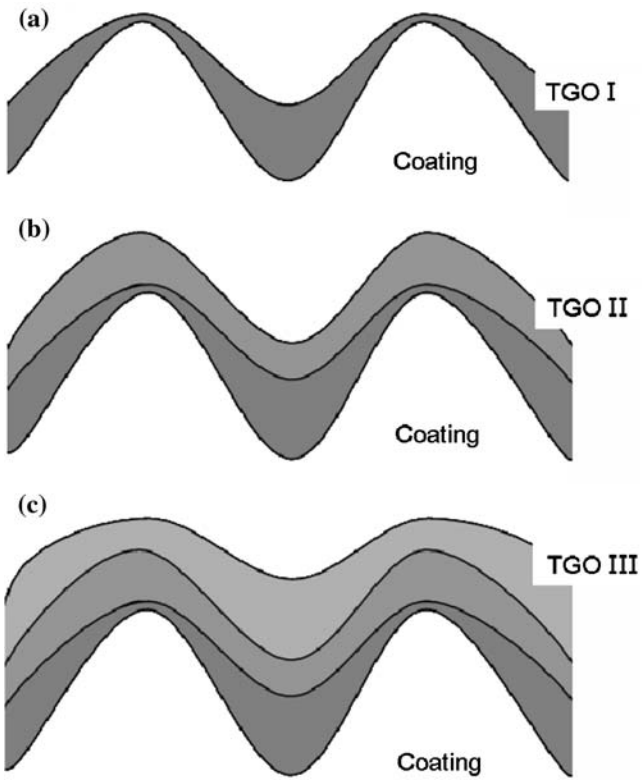

Fig. 7 Schematics of the surface roughness evolution with TGO growth

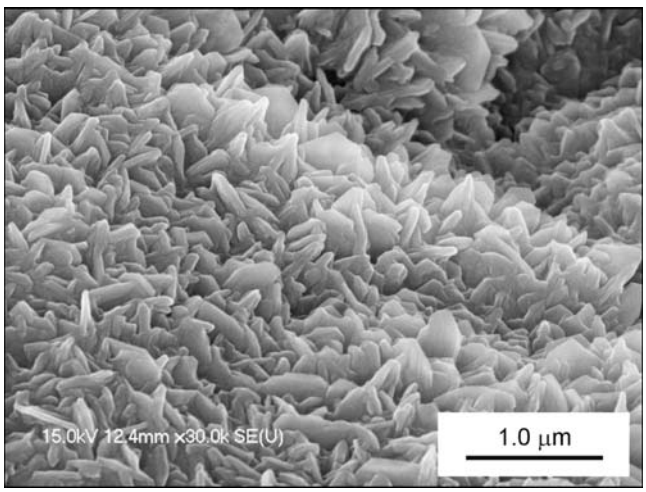

Fig. 8 SEM micrographs of the grown oxides (Al_2O_3) on the surface after 1 h thermal exposure

the thermal spray deposits after thermal exposure as shown in Fig. 4. As a result of the progressing oxidation, Al is permanently removed from the coating, resulting in the formation of an Al depleted zone underneath the TGO, indicated by the dissolution of the Al rich β phase. Figure 4(a) shows the β phase depleted zone underneath the TGO after 100 h exposure. In this case, the TGO is

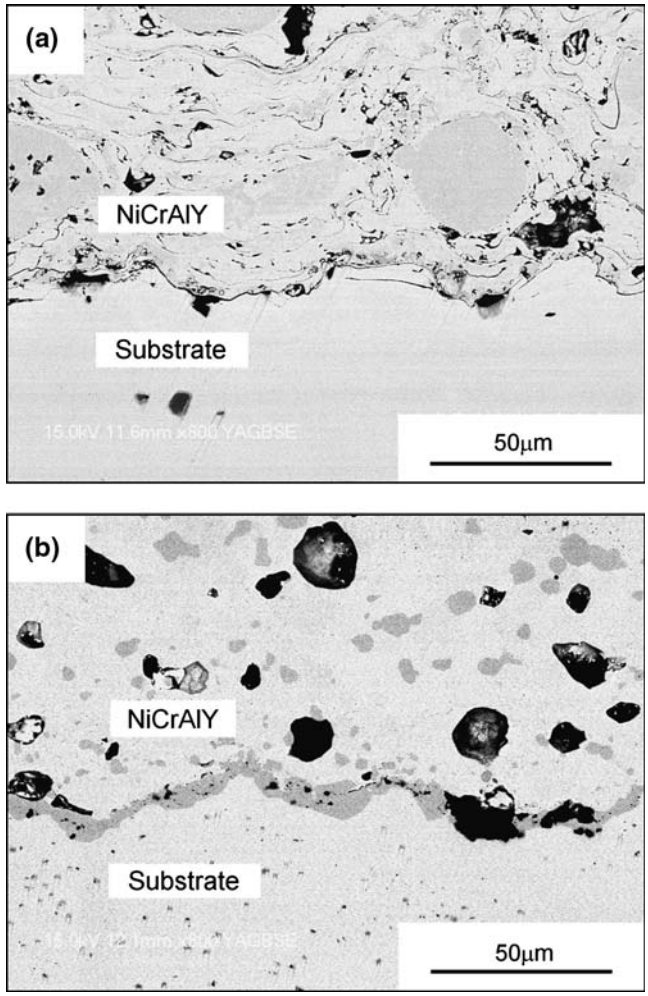

Fig. 9 Transformation of the interfacial microstructure of (a) as-sprayed and (b) 1,000 h-exposed coatings

relatively thin and sufficient Al is still available, as indicated by a relatively thin β phase depleted zone. The depth of the Al depletion in the coating will increase parabolically with the evolution of thermal exposure time (Ref 16). After 500 h thermal exposure, the microhardness values decreased once more, because the β phase depleted zone grew over the measuring area (average 100 μm from the surface), as shown in Fig. 4(b).

The elastic modulus of coating changed rapidly after thermal exposure as shown in Fig. 3, and then exhibited a tendency to have almost constant value with increasing of exposure time over 1 h. In general, the thermal spray coatings have the reduced E values, compared to the bulk materials (Ref 17). It is attributed to the unique microstructure of thermal spray deposits; i.e., the shape of lamella, weak interlamellar boundaries, interlamellar pores, and vertical cracks (intralamella cracks). After thermal exposure, the elastic modulus increased; meanwhile, H/E decreased. It can be deduced that the VPS NiCrAlY deposits behave more plastically after thermal exposure, although the E values increased. The evaluation of the

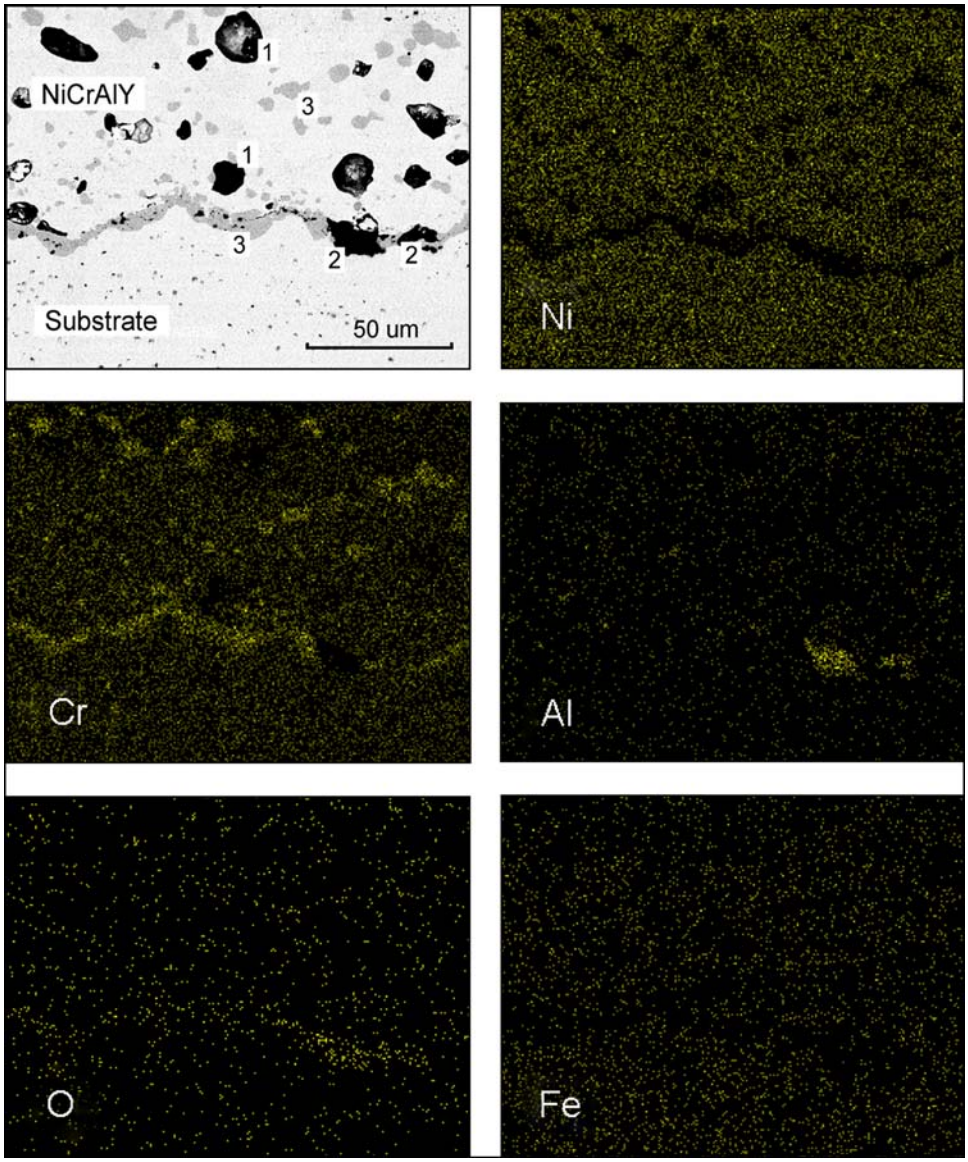

Fig. 10 EDX analysis of the 1,000 h thermal exposed coating; (1) diffusion cavity, (2) Al-O compound, and (3) Cr-rich (dark gray-colored) region

ratio of hardness to elastic modulus (H/E) is performed by measuring elastic recovery of indentations (Ref 17). H/E ratio is an expression based on a plastic-elastic model which relates the elastic depth recovery of the Vickers indentation to H/E. Elastic recovery occurs after the unloading half-cycle of indentation. The term H/E can be considered as a useful indicator to represent the degree of elastic response in elastic-plastic materials; i.e., H/E is small for rigid/plastic materials and becomes larger for more-elastic materials.

3.2 Evolution of Surface Roughness

Figure 5 shows the surface roughness of as-sprayed and exposed coatings with increasing exposure time. The surface roughness generally increases with increasing the particle size of starting powder (Ref 13-15). The surface roughness of NI-343 decreased up to stage I (1-10 h after thermal exposure) with increasing exposure time, beyond stage I surface roughness was increased slightly or kept in relatively fixed value (7.5-8 μm). This could be due to the partial sintering effect of inter-splat pores at the time of stage I (Ref 8). Another possible explanation may be the growth of Al_2O_3 on the surface as shown in Fig. 6. The open pores of surface could be filled with these oxides (TGO I) at first stage of exposure as shown in Fig. 6(a). The oxide scale was concentrated in the valley of surface at first 1 h exposure, as shown in Fig. 7(a). At next stage from 10 to 100 h, oxide scales (TGO II) also grew on the convex surface (hill-side) as shown in Fig. 6(b), leading to

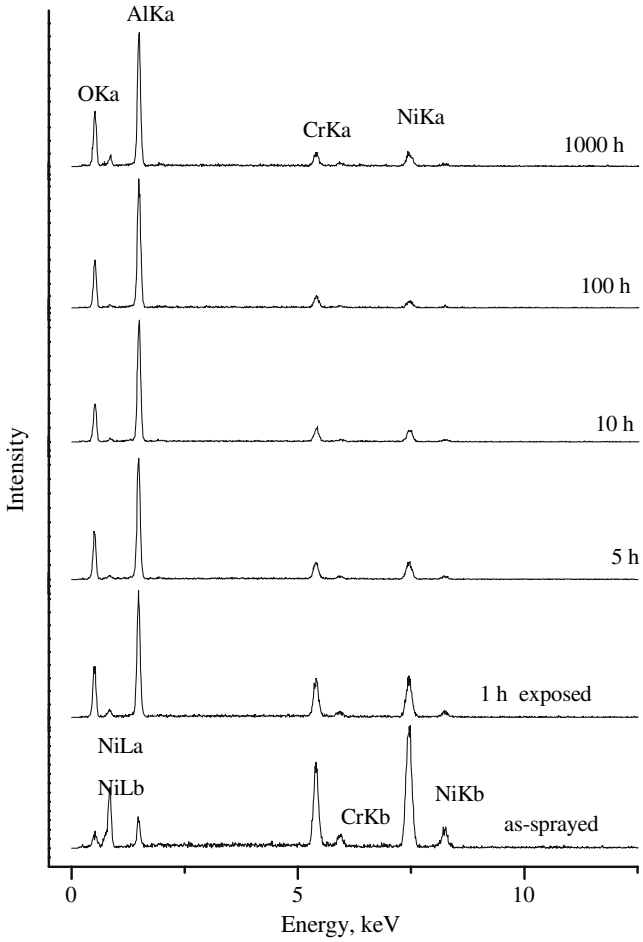

Fig. 11 EDX spectra of the NI-343 coating according to exposure time

increased surface roughness (refer to Fig. 7b). Finally the roughness decreased again due to growth of additional scales (TGO III) as shown in Fig. 6(c) and 7(c). The grown scale is relatively fine compared to the concavo-convex curvature of the as-sprayed surfaces, as shown in Fig. 8, so the thermal-exposed surface becomes smoother and more fine-grained gradually.

3.3 Oxidation Behavior

Figure 9 shows the cross-sectional morphologies of the interfaces between NiCrAlY coatings and substrates after as-sprayed and 1,000 h exposure. An explanation of the intergranular voids present in the scale was given by Choi (Ref 18). In the absence of the effective sinks for vacancies, vacancies generated by outward diffusion of alloying elements such as Ni and Cr condense to form cavities as shown in Fig. 10. One of the most effective methods to develop oxidation resistance in alloys and coatings at temperatures above about 1,223 K is to form continuous scales of α-Al_2O_3 via selective oxidation. As the oxidation time increases, transient oxidation stage is suppressed and then a protective alumina oxide layer is formed. The following processes are highly dependent on the oxidation temperature and microstructures of VPS MCrAlY coatings;

- Al depletion
- Ni outward diffusion
- Ni solid state reaction with pre-existing alumina to form spinel phase
- Cr_2O_3 oxide formation at the oxide-metal interface.

From the previous research, the sectional porosity including the diffusion cavities was affected by the sintering effect at the first exposure stage, but after this stage it was affected by the effect of grain overgrowth (Ref 19). It can also be found that the coating was deposited by partially melted particles, which correspond to the microstructure of the stacking of the particles in elliptical or spherical shapes. The failure of the coating system occurred by decohesion of the oxide scale at the oxide-metallic coat interface, and coatings was found to be degraded by oxidation and interdiffusion with the alloy substrate permitting the formation of nonprotective oxide scale near the coating surface.

From the results of EDX analysis of the NI-343 coating according to the thermal exposed time, there were metallic phases composed mainly of Ni, Cr, and Al on the as-sprayed coating, as shown in Fig. 11. In the case of exposed coatings at 1,273 K, the major metallic elements, i.e., Cr and Ni decreased, but Al and O increased gradually according to increasing exposure time. This phenomenon represents the growth of Al_2O_3 oxides. But, over 5 h exposure, all peaks of elements have become stable relatively. The stable Cr and Ni element peaks in high exposure time region represent the additional oxide growth. These Cr-O or Ni-Cr-O systems represent the development of typical mixed oxides at the latter thermal exposure stage. In Ni-base MCrAlY coatings such as NiCrAlY, Ni elements might lead to decrease of mixed oxide scale formation relatively. In case of CoNiCrAlY coatings, over 100 h exposures, Cr and Co elements have become much richer than Al (Ref 19). This represents the full-developed and richer mixed oxides as compared with NiCrAlY coatings.

4. Conclusions

Structural transformation behaviors of the VPS NiCrAlY metallic overlay coatings were observed under isothermal oxidation condition. Coating was oxidized isothermally at 1,273 K for different times in order to form a TGO layer. The TGO formation on coatings was considerably influenced by the exposure time, microstructure, and chemical composition. The square value of TGO thickness was proportional to the exposure time, and the square of weight gain was also proportional to the exposure time. The surface roughness and hardness decreased after isothermal exposure, but they are not proportional to the exposure time. The oxide scales were concentrated in

the valley of surface at the early 1 h exposure. The oxide scales grew on the convex surface from 10 h, and so the surface roughness increased. Finally the surface roughness decreased again.

Acknowledgments

This work was partially supported by the Korea Research Foundation Grant funded by the Korean Government (MOEHRD) (KRF-2005-214-D00219).

References

1. N. Briks and G.H. Meier, *Introduction to High Temperature Oxidation of Metals*, Edward Arnold, 1983
2. P. Kofstad, *High Temperature Oxidation of Metals*, Wiley, 1966
3. P. Kofstad, *High Temperature Corrosion*, Elsevier, 1988
4. A.S. Khanna, *Introduction to High Temperature Oxidation and Corrosion*, ASM International, 2002
5. K. Shimotor and T. Aisaka, The Trend of MCrAlX Alloys for High-temperature-protective Coatings, *Tetsu To Hagane-J. Iron Steel Inst. Jpn.*, 1983, **69**(10), p 1229-1241, in Japanese
6. M.J. Pomeroy, Coatings for Gas Turbine Materials and Long Term Stability Issues, *Mater. Des.*, 2005, **26**, p 223-231
7. J.M. Guilemany, J. Nutting, J.R. Miguel, and Z. Dong, Microstructure Characterization of WC-NI Coatings obtained by HVOF Thermal Spraying, *Scripta Metall. Mater.*, 1995, **33**(1), p 55-61
8. K. Ogawa, K. Ito, T. Shoji, D.W. Seo, H. Tezuka, and H. Kato, Effects of Ce and Si Additions to CoNiCrAlY Bond Coat Materials on Oxidation Behavior and Crack Propagation of Thermal Barrier Coatings, *J. Therm. Spray Technol.*, 2006, **15**(4), p 640-651
9. J.R. Nicholls, N.J. Simms, W.Y. Chan, and H.E. Evans, Smart Overlay Coatings – Concept and Practice, *Surf. Coat. Technol.*, 2002, **149**(2-3), p 236-244
10. L. Ajdelsztajn, F. Tang, G.E. Kim, V. Provenzano, and J.M. Schoenung, Synthesis and Oxidation Behavior of Nanocrystalline MCrAlY Bond Coatings, *J. Therm. Spray Technol.*, 2005, **14**(1), p 23-30
11. N. Birks, G.H. Meier, and F.S. Pettit, Forming Continuous Alumina Scales to Protect Superalloys, *JOM-J. Min. Met. Mat. S.*, 1994, **46**(12), p 42-46
12. A.M. Huntz, Stresses in NiO, Cr_2O_3 and Al_2O_3 Oxide Scales, *Mater. Sci. Eng. A-Struct. Mater. Prop. Microstruct. Process.*, 1995, **201**(1-2), p 211-228
13. N. Czech, M. Juez-Lorenzo, V. Kolarik, and W. Stamm, Influence of the Surface Roughness on the Oxide Scale Formation on MCrAlY Coatings Studied In situ by High Temperature X-ray Diffraction, *Surf. Coat. Technol.*, 1998, **108**(1-3), p 36-42
14. M.P. Taylor and H.E. Evans, The Influence of Bond Coat Surface Roughness and Structure on the Oxidation of a Thermal Barrier Coating System, *Mater. Sci. Forum*, 2001, **369**(3), p 711-717
15. U. Bardi, L. Carrafiello, R. Groppetti, F. Niccolai, G. Rizzi, A. Scrivani, and F. Tedeschi, On the Surface Preparation of Nickel Superalloys before CoNiCrAlY Deposition by Thermal Spray, *Surf. Coat. Technol.*, 2004, **184**(2-3), p 156-162
16. H. Echsler, D. Renusch, and M. Schutze, Bond Coat Oxidation and Its Significance for Life Expectancy of Thermal Barrier Coating Systems, *Mater. Sci. Technol.*, 2004, **20**, p 307-318
17. S.H. Leigh, C.K. Lin, and C.C. Berndt, Elastic Response of Thermal Spray Deposits under Indentation Tests, *J. Am. Ceram. Soc.*, 1997, **80**(8), p 2093-2099
18. H.S. Choi, B. Yoon, H.J. Kim, and C.H. Lee, Isothermal Oxidation of Air Plasma Spray NiCrAlY Bond Coatings, *Surf. Coat. Technol.*, 2002, **150**(2-3), p 297-308
19. D. Seo, K. Ogawa, M. Tanno, T. Shoji, and S. Murata, Influence of Heat Exposure Time on Isothermal Degradation of Plasma Sprayed CoNiCrAlY Coatings, *Surf. Coat. Technol.*, 2007, **201**(18), p 7952-7960